

Optical anisotropy of ellipsoidal quantum dots

G. Cantele, G. Piacente,* D. Ninno, and G. Iadonisi

*Istituto Nazionale per la Fisica della Materia and Università di Napoli "Federico II"—Dipartimento di Scienze Fisiche,
Complesso Universitario Monte S. Angelo, Via Cintia, I-80126 Napoli, Italy*

(Received 19 March 2002; published 23 September 2002)

The optical properties of anisotropic quantum dots with ellipsoidal shape are investigated and discussed as a function of the dot aspect ratio. The energy spectrum (ground and many excited states) is calculated and analyzed in comparison with the spherical quantum dot. The optical matrix elements in the dipole approximation and the oscillator strengths for the infrared transitions are shown. The main result is that optical processes significantly depend on the radiation polarization in contrast to nonpolarized processes observed for spherical quantum dots. The dot anisotropy is shown to play a fundamental role in determining the dot properties.

DOI: 10.1103/PhysRevB.66.113308

PACS number(s): 73.22.Dj, 78.67.Bf, 78.67.Hc

I. INTRODUCTION

The study of confined systems from both the theoretical and the experimental point of view, has attracted the attention of many scientists, mainly because new properties occur when dimensions are reduced down to nanometric scale, as effect of quantum confinement. For such systems atomiclike features can be reproduced, with a very wide range of applications, mostly due to the possibility of a size-tunable response.¹⁻³

Recent experimental works^{4,5} have demonstrated that the tuning of the optical properties can be further extended if control can be reached on the system shape. Anisotropic quantum dots (quantum rods) have been realized, by chemically controlling the nanostructure aspect ratio. This gives rise, for example, to radiation emission that becomes strongly linearly polarized, in contrast to nonpolarized radiation arising from spherical quantum dots, rendering these systems very useful in many optical emitter applications.⁶

In previous works⁷⁻⁹ we have shown that if an ellipsoidal quantum dot with azimuthal symmetry is considered, the single-particle effective-mass Schrödinger equation can be exactly solved by introducing a suitable coordinates system in which it is separable (just as for the spherical quantum dot). This allows the study (even if in the simplest, effective-mass scheme) of anisotropy-dependent features, with the possibility of accounting for arbitrarily anisotropic systems. The single-particle wave functions and eigenvalues have been calculated for the ground and the first excited states,^{7,8} bringing out the main differences that arise with respect to the spherical quantum dot. Moreover, some results concerning the dependence of the system optical properties on the anisotropy have been presented for prolate ellipsoidal quantum dots,⁸ showing how the observed emission and absorption spectra should be dependent on the radiation polarization. Finally, two-particle features have been studied,⁹ showing how the spatial configuration of two electrons within the ellipsoidal dot as well as the electron-electron correlation depends on the anisotropy. Some interesting features of anisotropic nanostructures can also be found in Ref. 10, where the quantum dot ellipsoidal geometry is studied within the perturbation theory as a deformation with respect to the spherical dot and in Ref. 11, where two-dimensional elliptic

quantum dots and elliptic quantum wires are studied, including the finite potential barrier at the boundary.

In this paper, we want to give a more complete overview on how by varying the system aspect ratio its properties significantly modify, giving rise to a very complicated spectrum. The single-particle energy spectrum is exactly calculated up to 10 excited states as a function of the dot aspect ratio. The removal of some degeneracies as well as the appearance of new ones are discussed (Sec. II). Infrared optical transitions are investigated both for prolate and oblate ellipsoidal dots. The study of both the optical matrix elements and the oscillator strength in the dipole approximation shows interesting features induced by the dot shape (Sec. III).

II. THE SINGLE-PARTICLE SPECTRUM

Let us consider an ellipsoidal quantum dot with rotational symmetry around a given axis (the z axis) and call c and a its axes along the z and x - y directions, respectively. In the following the ellipsoid aspect ratio will be indicated by $\chi = c/a$ ($\chi > 1$ for prolate ellipsoids, $\chi < 1$ for oblate ellipsoids). In previous works⁷⁻⁹ we have shown that it is possible to give a formally exact solution for the effective-mass Schrödinger equation for a particle moving within this dot by performing the transformation to *prolate spheroidal coordinates* or *oblate spheroidal coordinates*,¹²⁻¹⁴ depending on whether $c > a$ or $c < a$, respectively. This transformation $(x, y, z) \rightarrow (\xi, \eta, \varphi)$ allows wave function separation in the form $\Psi_{nlm}(\vec{r}) = \mathcal{A}_{nlm} j_{lm}(\xi) S_{lm}(\eta) \exp(im\varphi)$, where \mathcal{A}_{nlm} is a normalization constant and $n = 1, 2, \dots$, $m = 0, \pm 1, \dots$, and $l = |m|, |m| + 1, \dots$; j and S will be referred to, for analogy to the spherical quantum dot, as the “radial” and angular part of the wave function. The corresponding eigenvalues can be put in the form $E_{nlm} = (\hbar^2/2m^*c^2) \varepsilon_{nlm}(\chi)$, where m^* is the particle effective mass and $\varepsilon_{nlm}(\chi)$ an adimensional quantity depending just on the ellipsoid aspect ratio, but not on a and/or c separately.

The ellipsoid quantum dot spectrum has been calculated for both prolate ($\chi > 1$) and oblate ($\chi < 1$) ellipsoidal quantum dots. It is shown respectively in Fig. 1 (in units of $\hbar^2/2m^*a^2$) and in Fig. 2 (in units of $\hbar^2/2m^*c^2$). The spherical quantum dot degeneracy with respect to m is removed, as effect of the loss of spherical symmetry. At the same time,

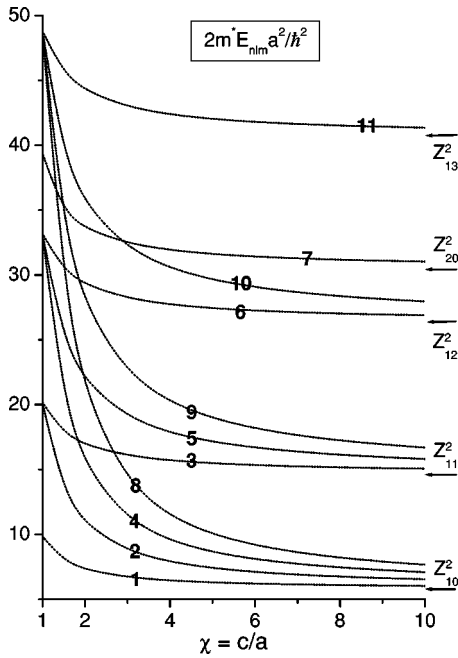


FIG. 1. The prolate ellipsoid quantum dot spectrum as a function of χ . The energies are calculated with fixed a and are shown in units of $\hbar^2/2m^*a^2$. The arrows indicate miniband edges of a cylindrical quantum wire of radius a (Z_{ns} is the n th zero of the s th cylindrical Bessel function). Legend: (1) 100; (2) 110; (3) 11 ± 1 ; (4) 120; (5) 12 ± 1 ; (6) 12 ± 2 ; (7) 200; (8) 130; (9) 13 ± 1 ; (10) 13 ± 2 ; (11) 13 ± 3 .

accidental degeneracies (levels crossings) appear. It is clear that the dot anisotropy plays a central role in determining the transition energies and it is expected to strongly influence the dot optical response.

The spherical quantum dot limit is retrieved as $\chi \rightarrow 1$. For many values of n, l and m it has been numerically checked that this limit is verified very accurately. In this case the typical scaling of the confined eigenvalues with $V^{-2/3}$ (where V is the system volume) is retrieved.

As already mentioned above, levels crossings appear for both prolate and oblate ellipsoids. In particular, it is seen that if $\chi > 1$ the states with the same n and m but different l become almost degenerate as large values of χ are considered (see Fig. 1). Similarly, as χ approaches zero, states with the same n group into two sets of almost degenerate states, each set containing all the states with odd or even value of $l-m$ (see Fig. 2). An explanation can be given by considering that if with fixed a we increase χ or, equivalently, c (prolate ellipsoids), more and more elongated quantum rods are obtained, the limit geometry for $\chi \rightarrow +\infty$ being a cylindrical quantum wire with radius a . A miniband energy structure appears, with the edge of each miniband depending on the two quantum numbers n (related to the number of nodes of the radial part of the wave function) and m ($m\hbar$ being the z component of the particle angular momentum). On increasing c , each ellipsoid confined state changes continuously in such a way that its limit is just a cylindrical quantum wire state having the same m and the same number of nodes of the wave function along the radial coordinate. All the ellipsoid

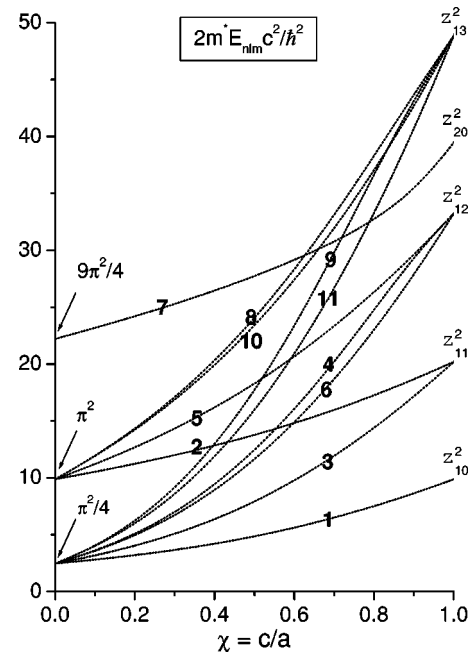


FIG. 2. The oblate ellipsoid quantum dot spectrum as a function of χ . The energies are calculated with fixed c and are shown in units of $\hbar^2/2m^*c^2$. z_{ns} is the n th zero of the s th spherical Bessel function. The arrows indicate miniband edges of a slab with distance $2c$. Legend: same as in Fig. 1.

quantum states with the same n and m but different l reconstruct a miniband of the cylindrical quantum wire, which explains why, for example, the states with $n=1, l=0,1,2,3, \dots, m=0$ (labeled as 1, 2, 4, 8, ... in Fig. 1) appear nearly degenerate as $c \rightarrow +\infty$. In the same way it can be explained the electronic spectrum structure if with fixed c ellipsoids with smaller and smaller χ are considered (that is, with increasing a). In this case the limit structure is given by two parallel planes (slab) with distance $2c$. The family of states $\{|nlm\rangle\}_{l=0,1,2, \dots}$ reconstruct, in the limit $\chi \rightarrow 0$, two slab minibands, corresponding to quantum states with different parity. Therefore, starting from the spherical quantum dot spectrum (obtained with $c=a$) and by increasing or decreasing χ , it has to be modified in such a way to reproduce the cylindrical quantum dot spectrum for large values of χ or the slab spectrum for small values of it. Because the energy levels in the two spectra are differently ordered, the appearance of levels crossings is needed, which explains the presence of accidental degeneracies. All these results bring out a very strong dependence of the system electronic properties on the dot anisotropy.^{7,8}

It can be useful to get interpolation formulas for the quantum confined energy levels. It has been found that the following equations interpolate the numerical results within 0.4% for $0.5 \leq \chi \leq 5.0$:

$$\varepsilon_{100}(\chi) = 2.97035 + 6.59569(\chi + 0.02361)^{1.95395}, \quad (1a)$$

$$\varepsilon_{110}(\chi) = 11.0548 + 8.20660(\chi + 0.05827)^{1.88390}, \quad (1b)$$

$$\varepsilon_{111}(\chi) = 3.16983 + 15.71608(\chi + 0.0416)^{1.97543}. \quad (1c)$$

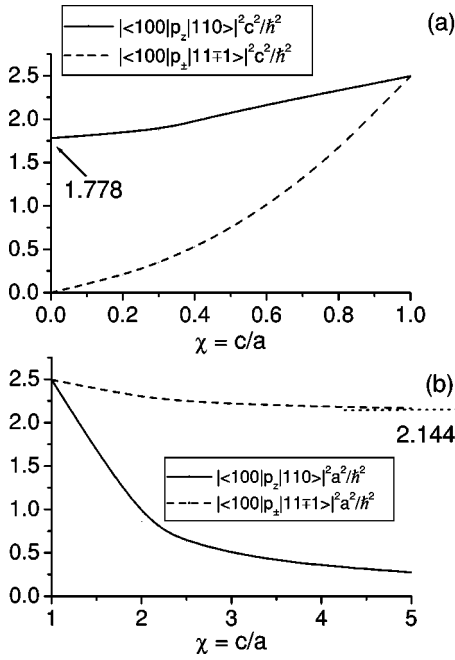


FIG. 3. The square modulus of the momentum operator matrix elements $[p_{\pm} = (p_x \pm ip_y)/\sqrt{2}]$ as a function of the dot aspect ratio for both (a) $\chi < 1$ (in units of \hbar^2/c^2) and (b) $\chi > 1$ (in units of \hbar^2/a^2). The limits $\chi \rightarrow 0$ and $\chi \rightarrow \infty$ reproduce the corresponding matrix elements for the slab and the cylindrical quantum wire, respectively (see text).

III. INFRARED PROPERTIES

The calculation of the quantum confined eigenvalues and eigenfunctions for an electron moving inside an ellipsoidal dot allows the investigation of some interesting features of the infrared (conduction-band) transitions in such systems. First of all, let us note that, while for the spherical quantum dot only transitions with $\Delta l = \pm 1$ are allowed, the lower degree of symmetry of the ellipsoid quantum dot relaxes this selection rule, making in principle allowed any transition for which Δl is odd. Moreover, the condition $\Delta m = 0, \pm 1$ still remains valid. Transitions with $\Delta m = 0$ involve radiation linearly polarized along the z axis, while transitions with $\Delta m = \pm 1$ radiation circularly polarized in the x - y plane.

The optical matrix elements have been calculated for both linearly polarized radiation along the z axis and circularly polarized radiation in the x - y plane relative to transitions from or to the ground state $|100\rangle$. In this case the allowed transitions are $|100\rangle \rightarrow |nlm\rangle$ with $l = 1, 3, 5, \dots$ and $|m| = 0, 1$. It is worth pointing out that if a given transition is allowed in the dipole approximation with linearly polarized light, it cannot be allowed with circularly polarized light and vice versa.

In Fig. 3 the square modulus of the momentum operator matrix element is shown for both (a) $\chi < 1$ (in units of \hbar^2/c^2) and (b) $\chi > 1$ (in units of \hbar^2/a^2). It is seen that the dot anisotropy makes the transitions with polarization along the ellipsoid major axis very different from those with polarization along the minor axis. This gives a clear evidence to the fact that by realizing anisotropic systems, polarization-dependent processes can be obtained. The more the dot geom-

etry is different from the spherical one, the more “anisotropic” is its response to polarized radiation. This result is related to the quantum states deformation due to the geometry, which leads to $n = 1, l = 1$ states whose spatial configuration is strongly dependent on m .⁸ Let us note, following the discussion presented above, that the transition $|100\rangle \leftrightarrow |110\rangle$ is forbidden as $\chi \rightarrow \infty$, because the two states have the same n and m so they belong to the same cylinder miniband in the considered limit. Similarly, the transition $|100\rangle \leftrightarrow |11\pm 1\rangle$ is forbidden as $\chi \rightarrow 0$ because the two states have the same n and $l - |m|$ so they belong to the same slab miniband. This is confirmed by the fact that the corresponding matrix elements of the momentum operator go to zero in the respective limits. In the opposite limits the two transitions correspond to the first miniband-miniband allowed transition in the two limit structures and the corresponding square matrix elements of the momentum operator are $1.778\hbar^2/c^2$ (radiation linearly polarized along the z axis in the slab limit $\chi \rightarrow 0$) and $2.144\hbar^2/a^2$ (radiation circularly polarized in the x - y plane in the cylinder limit $\chi \rightarrow \infty$). This two limits are perfectly verified by our numerical results (see Fig. 3). It is possible to get simple interpolation formulas for the momentum matrix elements $[p_{\pm} = (p_x \pm ip_y)/\sqrt{2}]$ for both $\chi > 1$,

$$\begin{aligned} | \langle 100 | p_z | 110 \rangle |^2 &= (\hbar^2/a^2) [0.13743 + 12.78957 \\ &\times \exp(-\chi/0.46327) + 1.40263 \\ &\times \exp(-\chi/2.14216)], \end{aligned} \quad (2a)$$

$$\begin{aligned} | \langle 100 | p_{\mp} | 11\pm 1 \rangle |^2 &= (\hbar^2/a^2) [2.10966 + 0.90542 \\ &\times \exp(-\chi/0.65661) + 0.25467 \\ &\times \exp(-\chi/3.24178)], \end{aligned} \quad (2b)$$

and $\chi < 1$,

$$\begin{aligned} | \langle 100 | p_z | 110 \rangle |^2 &= (\hbar^2/c^2) [1.77777 - 0.54423\chi + 4.25123\chi^2 \\ &- 4.96969\chi^3 + 1.98035\chi^4], \end{aligned} \quad (2c)$$

$$\begin{aligned} | \langle 100 | p_{\mp} | 11\pm 1 \rangle |^2 &= (\hbar^2/c^2) [-3.70736 \times 10^{-4} + 0.84914\chi + 0.49526\chi^2 \\ &+ 1.97488\chi^3 - 0.82208\chi^4]. \end{aligned} \quad (2d)$$

These formulas hold in the intervals $1 \leq \chi < 5$ and $0 \leq \chi < 1$, respectively, and reproduce our numerical results within at most 1.0%. Let us note that from Eqs. (1) and (2) it is in principle possible to build all the relevant infrared optical properties of the ellipsoidal quantum dot (absorption coefficient, dielectric function, etc.).

In Fig. 4 the oscillator strengths relative to the the same transitions are shown. It comes out that there is not a very strong variation with the dot geometry, unless very anisotropic systems are considered. If the oscillator strengths sum rule is performed for the transitions from the ground state to the three states with $n = l = 1$, values of about 0.96 are obtained. If the transitions towards the states with $n = 1, l = 3$ are included, the value of the sum becomes about 0.99. This clearly shows how for confined systems the oscillator

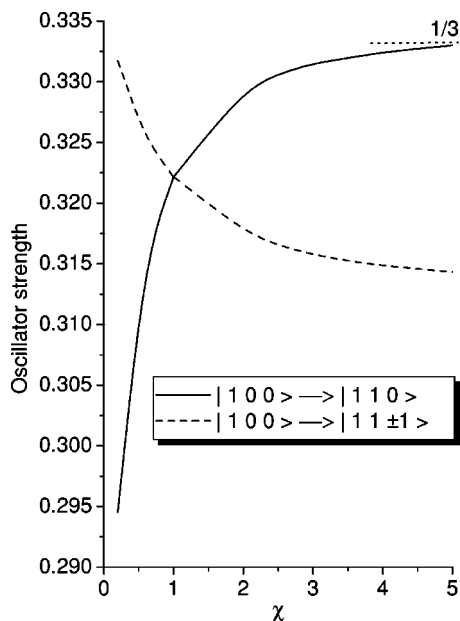


FIG. 4. The oscillator strengths relative to the first two allowed infrared transitions.

strengths become concentrated over very few, sharp transitions. This is confirmed by the calculation of the square modulus of the matrix elements of the momentum operator, relative to the transitions from the ground state to the states $|13m\rangle$. Results of one or two order of magnitude smaller than those shown in Eqs. (2) are obtained. This reflects the smaller transition probability but, on the other hand, demonstrates the presence of optical transitions forbidden for the spherical dot.

IV. CONCLUSIONS

In this work optical properties of ellipsoidal quantum dots have been discussed. By exactly solving the effective-mass, single-particle Schrödinger equation as shown elsewhere,⁷ the full electronic spectrum has been calculated, showing the

primary role played by the dot shape. The removal of degeneracies with respect to the spherical dot as well as the appearance of levels crossings have been brought out. Experimental evidences for degeneracy splittings have been found by using femtosecond pump-probe transient spectroscopy on CdSe nanorods.¹⁵

From all these results, it comes out that the fabrication of shape-controlled ellipsoid quantum dots can have fundamental applications. First, the infrared transition energies can be tuned as a function of both the dot shape and dimensions, giving the possibility of tuning the system resonant frequency even keeping constant the dot volume. In other words, asymmetric quantum dots can be realized, with the infrared absorption peak at any infrared wavelength. Second, the control on the ellipsoid aspect ratio allows the fabrication of nanostructures which exhibit light emission and absorption spectra dependent on the radiation polarization. The study presented in this work has been focused on the infrared spectrum, for which experimental data are now becoming available.¹⁶ Moreover, experiments done on the photoluminescence emission of anisotropic dots have given a clear evidence for such applications. In particular, single-molecule luminescence spectroscopy measurements on CdSe quantum rods have shown a sharp transition from nonpolarized to purely linearly polarized emission if the ellipsoid aspect ratio is varied from 1 to 2, making these nanocrystals ideal for many orientation-sensitive applications.⁶ In the same way, it has been shown how by fixing the minor axis a and changing only the major axis c , the emission wavelength can be tuned over the same range as for spherical quantum dots, while the emission from each individual CdSe quantum rod is highly linearly polarized in contrast to the plane-polarized emission from spherical dots.¹⁷

ACKNOWLEDGMENTS

G. Cantele has been supported by the European Social Found. Financial support from ENEA under Contract No. 2000/29324 is acknowledged. We wish to thank F. M. Peeters for a critical reading of the manuscript.

*Present address: Department of Physics, Universiteit Antwerpen, Universiteitsplein 1, B-2610 Antwerpen, Belgium.

¹A.P. Alivisatos, *J. Phys. Chem.* **100**, 13226 (1996) and references therein.

²P. Moriarty, *Rep. Prog. Phys.* **64**, 297 (2001) and references therein.

³A.D. Yoffe, *Adv. Phys.* **50**, 1 (2001) and references therein.

⁴X.G. Peng, L. Manna, W. Yang, J. Wickham, E. Scher, A. Kadavanich, and A.P. Alivisatos, *Nature (London)* **404**, 59 (2000).

⁵V.F. Puntès, K.M. Krishnan, and A.P. Alivisatos, *Science* **291**, 2115 (2001).

⁶J. Hu, L.-s. Li, W. Yang, L. Manna, L.-w. Wang, and A.P. Alivisatos, *Science* **292**, 2060 (2001).

⁷G. Cantele, D. Ninno, and G. Iadonisi, *J. Phys.: Condens. Matter* **12**, 9019 (2000). In Fig. 2 of this paper the curve relative to the state with $l=1$, $m=0$ is not correct in the range $0 < \chi < 1$. Actually, this curve tends, as $\chi \rightarrow 0$, to π^2 (see Fig. 2 of this work).

⁸G. Cantele, D. Ninno, and G. Iadonisi, *Nano Lett.* **1**, 121 (2001).

⁹G. Cantele, D. Ninno, and G. Iadonisi, *Phys. Rev. B* **64**, 125325 (2001).

¹⁰A.L. Efros and A.V. Rodina, *Phys. Rev. B* **47**, 10 005 (1993).

¹¹M. van den Broek and F.M. Peeters, *Physica E (Amsterdam)* **11**, 345 (2001).

¹²P. M. Morse and H. Feshbach, *Methods of Theoretical Physics* (McGraw-Hill, New York, 1953).

¹³J. A. Stratton, P. M. Morse, L. J. Chu, J. D. C. Little, and F. J. Corbatò, *Spheroidal Wave Functions* (Wiley, New York, 1956).

¹⁴M. Abramovitz and I. A. Stegun, *Handbook of Mathematical Formulas* (Dover, New York, 1972).

¹⁵M.B. Mohamed, C. Burda, and M.A. El-Sayed, *Nano Lett.* **1**, 589 (2001).

¹⁶M. Shim and P. Guyot-Sionnest, *Nature (London)* **407**, 981 (2000).

¹⁷L.-s. Li, J. Hu, W. Yang, and A.P. Alivisatos, *Nano Lett.* **1**, 349 (2001).